Automatika

Journal for Control, Measurement, Electronics, Computing and Communications

ISSN: 0005-1144 (Print) 1848-3380 (Online) Journal homepage: https://www.tandfonline.com/loi/taut20

Dynamic characteristic analysis of replenishing/leaking parallel valve control systems

Haigang Ding & Jiyun Zhao

To cite this article: Haigang Ding & Jiyun Zhao (2017) Dynamic characteristic analysis of replenishing/leaking parallel valve control systems, Automatika, 58:2, 182-194, DOI: 10.1080/00051144.2017.1386750

To link to this article: https://doi.org/10.1080/00051144.2017.1386750

AUTOMATIKA, 2017
VOL. 58, NO. 2, 182–194
https://doi.org/10.1080/00051144.2017.1386750

REGULAR PAPER

OPEN ACCESS Check for updates

Dynamic characteristic analysis of replenishing/leaking parallel valve control systems

Haigang Ding[a] and Jiyun Zhao[b]

[a]School of Mechatronic Engineering, China University of Mining and Technology (CUMT), Xuzhou, China; [b]Jiangsu Key Laboratory of Mine Mechanical and Electrical Equipment, China University of Mining and Technology (CUMT), Xuzhou, China

ABSTRACT

To improve the dynamic response of traditional pump control systems, this paper proposes two new control schemes: replenishing parallel valve control (RPVC) and leaking parallel valve control (LPVC). A parallel valve control system using the two control schemes is designed, and its system parameters, control performances and efficiency are analysed and verified by simulation and experiments. Compared to the pump control system, the proposed system has larger damping ratios which vary widely with operating points, and has lower velocity stiffness due to the increase of total leakage coefficients. Both the LPVC and RPVC could contribute to the dynamic response improvement. RPVC is preferred over LPVC because of more stable damping ratios and higher speed stiffness, and these advantages could be further improved by increasing the supply pressure of the control valve, but the LPVC scheme costs lower due to the unnecessary oil supply for the control valve. During the control process, the valve works at a low flow rate, but the pump provides the majority of the system flow, so two parallel valve control systems still have relatively high energy efficiency with rapid response. Therefore, the RPVC and LPVC will enrich the control mode of hydraulic systems.

ARTICLE HISTORY
Received 22 June 2017
Accepted 26 September 2017

KEYWORDS
Rapid response; variable-speed pump control systems; parallel valve control; energy efficiency

1. Introduction

Traditional hydraulic control systems are of two basic types: pump control and valve control [1,2]. Valve control systems respond fast to valve and load inputs, but they are less efficient because of throttling loss and overflow loss [3]. Pump control systems usually are of two basic types: variable displacement pump control (VDPC) and variable-speed pump control (VSPC). They, respectively, control actuators by varying the stroke of a variable displacement pump and the rotary speed of a fixed displacement pump [4]. Compared with valve control systems, pump control systems are more efficient since both flow and pressure are closely matched with load requirements, but they have a critical drawback: slow response [1,2,4,5]. There are many reasons for this such as the slow response of the stroke mechanism in variable displacement pumps, high inertia of the pump and electric motor, and slow dynamic regulation of the electric motor due to the low overload capacity of its inverter. This disadvantage prevents pump control systems from being used in applications requiring a rapid response. Compared with the VDPC systems, the VSPC systems have many advantages such as better energy-saving, higher reliability and lower cost [5,6].

The valve–pump combination control includes two types: valve–pump serial control and valve–pump parallel control; they could take the advantages of pump control and valve control and could strike a balance between energy efficiency and dynamic response [7]. Dr Naseradinmousavi et al. focused on a novel nonlinear modelling and dynamic analysis of the actuated butterfly valves coupled in series [8], and study coupled operational optimization [9] and chaotic and hyperchaotic dynamics [10] of smart valve system subject to a sudden contraction. Manasek [11] proposed a valve–pump series variable-speed hydraulic system to accelerate the response of the pump control, where a flow control valve is installed in series on the main circuit. An energy-regulating device is added to the above system, and forms a variable-speed hydraulic system based on energy regulation [12–14]. The energy-regulation device can absorb redundant energy during the system deceleration, as well as release energy during the system acceleration; so the dynamic response of this system can be increased. Because the flow control valve limits the maximum flow of main circuit, the above serial control systems are unsuitable for large flow systems with high power. However, valve–pump parallel control systems could avoid this, where the flow control valve is mounted in parallel on the main circuit. Recently, a research of parallel control systems has mainly focused on electrohydraulic actuators [15–17], which are positioning servo devices. Moreover, these parallel control systems have one drawback in principle: there are no replenishing arrangements in such compound systems which are closed-cycle

CONTACT Haigang Ding haierdhg@126.com

systems, and the authors here try to control the actuator and replenish fluid in the system only by using the valve control branch circuit. In 2013 and 2014, Ding and Zhao proposed a hydraulic servo system in valve–pump parallel variable-structure control [18,19]. There are two control schemes: replenishing parallel valve control (RPVC) and leaking parallel valve control (LPVC), where a control valve could, respectively, work in the replenishing status and leaking status to regulate rapidly the system flow. In the valve–pump combined control system, RPVC is applied to achieve disturbance rejection at high speed, while the LPVC is applied to improve low-speed performance [20,21]. In this paper, the RPVC and LPVC are applied to improve the dynamic response of pump control systems while retaining a comparatively high efficiency. First, we design the parallel control system and explain its working principle, then build mathematical models and simulation models and analyse system parameters, control performance and efficiency before validating the results by step-response experiments. Of course, the control schemes are also available to VDPC systems.

2. Principle of new schemes

Figure 1 shows the schematic diagram of the parallel control system. In fact, the system is a closed hydraulic speed-regulation system and an individual replenishing arrangement is connected to the return chamber to compensate for the system leakage and maintain a constant chamber pressure.

The heat exchanger arrangement is made up of a hydraulic controlled direction valve and relief valve, and is necessary for closed hydraulic systems and is used to cool oil by exchanging hot fluid in the return chamber. Moreover, the arrangement also has an important function in the parallel system; it is used to put the redundant oil to the oil tank to balance the system flow. The fixed displacement pump supplies variable flow by changing the output frequency of the inverter. The proportional directional valve (PDV) is connected to the high-pressure chamber through a shuttle valve to drive the hydraulic motor with the pump, and could work in the replenishing status and leaking status according to control signals. The load pressure is controlled by a proportional relief valve (PRV). The speed of the hydraulic motor is measured and fed back to the controller via an encoder, and the controller outputs two control signals, one to the PDV to regulate its opening and another to the inverter to change the pump speed.

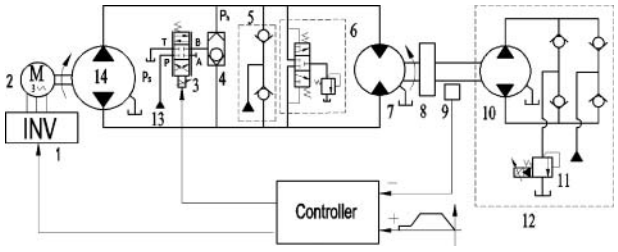

Figure 1. Schematic framework of parallel valve control system: 1 – Inverter; 2 – Electric motor; 3 – PDV; 4 – Shuttle valve; 5 – Replenishing arrangement; 6 – Heat exchanger arrangement; 7 – Hydraulic motor; 8 – Inertia; 9 – Encoder; 10 – Loading pump; 11 – PRV; 12 – Loading system; 13 – Oil source of PDV; 14 – Fixed displacement pump.

The compound system can work in the following three modes:

(1) In the VSPC mode, the PDV is closed with zero voltage, and the hydraulic motor speed varies with the inverter input, which could regulate the pump speed.
(2) In the RPVC mode, the pump discharges a certain amount of fluid flow at a fixed speed, which is less than the flow corresponding to the desired speed of the hydraulic motor. Meanwhile, the PDV is given a positive voltage and supplies fluid to the high-pressure chamber to compensate for the system leakage and to regulate the hydraulic motor speed.
(3) In the LPVC mode, the pump at a constant speed supplies a certain amount of flow, which is more than the required flow. Meanwhile, the PDV (with a certain pre-opening) is fed with a negative voltage to form a bypass leakage passage, and then the hydraulic motor speed is controlled by regulating the bypass leakage.

3. Mathematical modelling

3.1. Inverter–electric motor link

The inverter–electric motor link could be regarded as a first-order inertia element [18]:

$$n_p = \frac{K_u u_p - K_h P_h}{s/\omega_{bp} + 1} \tag{1}$$

where n_p is the electric motor speed, u_p is the inverter input voltage, K_u is the voltage coefficient, P_h is the high-pressure chamber pressure, K_h is the pressure coefficient proportional to pump the displacement D_p and ω_{bp} is the break frequency which is inversely proportional to the pump inertia.

Equation (1) indicates that n_p increases with increasing u_p and decreasing P_h. The actual flow of the pump Q_p is given by

$$Q_p = Q_{p0} - C_{tp} P_h \tag{2}$$

where C_{tp} is the pump total leakage coefficient, and $Q_{p0} = D_p n_p$ is the pump unload flow.

3.2. Bypass valve control circuit

The orifice equation of the valve PDV can be expressed as

$$Q_v = C_{sv} u_v \sqrt{\Delta P} \tag{3}$$

where C_{sv} is the valve constant and it goes together with the valve area gradient and fluid density, u_v is the control input and is proportional to spool displacement, and ΔP is the pressure drop across the valve.

Using a Taylor series, the linearized orifice equation of PDV is written as [1,2]

$$\begin{cases} Q_v = K_q u_v + K_c \Delta P \\ K_q = \dfrac{\partial Q_v}{\partial I_v} = C_{sv}\sqrt{\Delta P} \\ K_c = \dfrac{\partial Q_v}{\partial \Delta P} = \dfrac{C_{sv} u_v}{2\sqrt{\Delta P}} \end{cases} \tag{4}$$

where K_q is the flow gain of PDV and K_c is the flow-pressure gain of PDV.

In the LPVC mode, the PDV works in the leaking status, the pressure drop ΔP is P_h when ignoring the return pressure. So the linearized flow equation of the valve in the leaking status is

$$\begin{cases} Q_l = K_{ql} u_l + K_{cl} P_h \\ K_{ql} = C_{sv}\sqrt{P_h} \\ K_{cl} = \dfrac{C_{sv} u_l}{2\sqrt{P_h}} \end{cases} \tag{5}$$

where Q_l, K_{ql}, K_{cl} and u_l are flow, flow gain, flow-pressure gain and control input of the PDV in its leaking status, respectively.

In the RPVC mode, the valve works in the replenishing status and $\Delta P = P_s - P_h$, then the linearized flow equation of the valve at the replenishing status is

$$\begin{cases} Q_r = K_{qr} u_r - K_{cr} P_h \\ K_{qr} = C_{sv}\sqrt{P_s - P_h} \\ K_{cr} = \dfrac{C_{sv} u_r}{2\sqrt{P_s - P_h}} \end{cases} \tag{6}$$

where P_s is the supply pressure of the PDV, Q_r, K_{qr}, K_{cr} and u_r are the flow, flow gain, flow-pressure gain and control input of the PDV at replenishing status, respectively.

Considering the PDV as a second-order oscillating link, its unload flow in the leaking status is given by

$$Q_{v0} = \frac{K_q u_v}{\dfrac{s^2}{{\omega_{sv}}^2} + \dfrac{2\xi_{sv}}{\omega_{sv}} s + 1} \tag{7}$$

where ω_{sv} is the hydraulic natural frequency of the PDV and ξ_{sv} is its damping ratio.

From Equation 7, we can obtain the unload flow in the replenishing status Q_{r0}, when K_q is replaced by K_{qr} and u_v is replaced by u_r. In the same way, the unload flow in the leaking status Q_{l0} is obtained, when K_q is replaced by K_{ql} and u_v is replaced by u_l.

3.3. Valve–pump parallel control motor link

In the LPVC mode, the continuity equation for the whole system is

$$Q_p - Q_l = C_m P_h + D_m w_m + V_0 s P_h / \beta_e \tag{8}$$

In the RPVC mode, the continuity equation for the whole system is

$$Q_p + Q_r = C_m P_h + D_m w_m + V_0 s P_h / \beta_e \tag{9}$$

where w_m is the motor angular speed, C_m is the the motor leakage coefficient, D_m is the motor displacement and V_0 is the average volume of high-pressure chamber.

The torque balance equation for the hydraulic motor is

$$D_m P_h = J s w_m + B_m w_m + T_L \tag{10}$$

where J is the equivalent total inertia, B_m is the viscous damping coefficient, $T_L = D_L P_h$ is the load torque produced by the loading pump ignoring the low-pressure chamber pressure and $D_L = D_m$ is the displacement of the loading pump.

Combining Equations (2), (5), (7), (8) and (10), the open-loop dynamic equation in the LPVC mode is given by

$$w_m = \frac{\frac{Q_{p0} - Q_{l0}}{D_m} - \frac{C_l}{{D_m}^2}\left(1 + \frac{s}{2\omega_l \xi_l}\right) T_L}{\frac{s^2}{{\omega_l}^2} + \frac{2\xi_l}{\omega_l} s + 1} \tag{11}$$

where $C_l = C_p + C_m + K_{cl}$, $\omega_l = \sqrt{\frac{\beta_e {D_m}^2}{V_0 J}}$, $\xi_l = \frac{C_l}{2D_m}\sqrt{\frac{\beta_e J}{V_0}}$, C_l, ξ_l and ω_l are the total leakage coefficient, damping ratio and natural frequency in the LPVC mode, respectively.

Combining Equations (2), (6), (7), (9) and (10), the open-loop dynamic equation in the RPVC mode is given by

$$w_m = \frac{\frac{Q_{p0} + Q_{r0}}{D_m} - \frac{C_r}{{D_m}^2}\left(1 + \frac{s}{2\omega_r \xi_r}\right) T_L}{\frac{s^2}{{\omega_r}^2} + \frac{2\xi_r}{\omega_r} s + 1} \tag{12}$$

where $C_r = C_p + C_m + K_{cr}$, $\omega_r = \sqrt{\frac{\beta_e {D_m}^2}{V_0 J}}$, $\xi_r = \frac{C_r}{2D_m}\sqrt{\frac{\beta_e J}{V_0}}$, C_r, ξ_r and ω_r are the total leakage coefficient, damping ratio and natural frequency in the RPVC mode, respectively.

When the PDV is closed, and Q_{l0}, Q_{r0}, K_{cl} and K_{cr} are zero in Equations (11) and (12), the LPVC mode and RPVC mode will switch to the VSPC mode, and

its open-loop dynamic equation is [1,2,20]

$$w_m = \frac{\frac{Q_{p0}}{D_m} - \frac{C_t}{{D_m}^2}\left(1 + \frac{s}{2\omega_m \xi_m}\right) T_L}{\frac{s^2}{{\omega_m}^2} + \frac{2\xi_m}{\omega_m} s + 1} \tag{13}$$

where $C_t = C_p + C_m$, $\omega_m = \sqrt{\frac{\beta_e {D_m}^2}{V_0 J}}$, $\xi_m = \frac{C_t}{2D_m}\sqrt{\frac{\beta_e J}{V_0}}$, C_t, ξ_m and ω_m are the total leakage coefficient, damping ratio and hydraulic natural frequency in the VSPC mode, respectively.

The rotary component is simplified as a proportional element due to its fast response:

$$K_m = \frac{u_m}{n_m} \tag{14}$$

where u_m is the feedback voltage, K_m is the feedback gain and $n_m = 60w_m/(2\ \pi)$ is the motor angular velocity.

3.4. Total system mathematical model

Combining the above three links, the system block diagram in three modes is obtained as shown in Figure 2. Its uncompensated open-loop transfer functions are, respectively, given by

$$G_{mk}(s) = \frac{60K_m K_{v2}/(2\pi D_m)}{\left(\frac{s}{\omega_{bp}} + 1\right)\left(\frac{s^2}{{\omega_m}^2} + \frac{2\xi_m}{\omega_m} s + 1\right)} \tag{15}$$

$$G_{lk}(s) = \frac{60K_m K_{vl}/(2\pi D_m)}{\left(\frac{s^2}{{\omega_l}^2} + \frac{2\xi_l}{\omega_l} s + 1\right)\left(\frac{s^2}{{\omega_{sv}}^2} + \frac{2\xi_{sv}}{\omega_{sv}} s + 1\right)} \tag{16}$$

$$G_{rk}(s) = \frac{60K_m K_{vr}/(2\pi D_m)}{\left(\frac{s^2}{{\omega_r}^2} + \frac{2\xi_r}{\omega_r} s + 1\right)\left(\frac{s^2}{{\omega_{sv}}^2} + \frac{2\xi_{sv}}{\omega_{sv}} s + 1\right)} \tag{17}$$

Table 1 shows system parameters and indicates that $\omega_m = \omega_l = \omega_r < \omega_{bp} \ll \omega_{sv}$, so ω_m, ω_l and ω_r are the lowest break frequencies and it determines the dynamic system characteristics, and then ω_{sv} in Equations (16) and (17) can be omitted. Equations (15)–(17) show that three servo loops are Type 0 and

Table 1. System parameters.

Symbol	Value	Unit
V_0	1.0×10^{-3}	m^3
J	70	kg m^2
D_m	7.45×10^{-5}	m^3/rad
C_t	2.94×10^{-12}	m^3/(s Pa)
K_m	1/6	V min/r
ω_{bp}	16.7	rad/s
ω_{sv}	314	rad/s
ξ_{sv}	0.7	–
ω_m	10.48	rad/s
ξ_m	0.19	–
K_{vl} or K_{vr}	0.58	m^3/(s V)
C_l or C_r	$\geq 2.94 \times 10^{-12}$	m^3/(s Pa)
ω_l orω_r	10.48	rad/s
ξ_l orξ_r	≥ 0.19	–
K_1	2.14	–
K_2	3.10	–
K_3	3.10	–

unstable. We use a simply compensated internal method to correct three servo loops. Their compensated open-loop transfer functions are, respectively, given by

$$G_{mk}(s) = \frac{K1}{s\left(\frac{s}{\omega_{bp}} + 1\right)\left(\frac{s^2}{{\omega_m}^2} + \frac{2\xi_m}{\omega_m} s + 1\right)} \tag{18}$$

$$G_{lk}(s) = \frac{K_2}{s\left(\frac{s^2}{{\omega_l}^2} + \frac{2\xi_l}{\omega_l} s + 1\right)} \tag{19}$$

$$G_{rk}(s) = \frac{K_3}{s\left(\frac{s^2}{{\omega_r}^2} + \frac{2\xi_r}{\omega_r} s + 1\right)} \tag{20}$$

where $K_1 = 60K_{mI}K_{v2}K_m/(2\pi D_m)$, $K_2 = 60K_{lI}K_{vl}K_m/(2\pi D_m)$, $K_3 = 60K_{rI}K_{vr}K_m/(2\pi D_m)$ are compensated open-loop gains when the system is, respectively, in the VSPC, LPVC and RPVC modes, and K_{mI}, K_{lI} and K_{rI} are the internal gains in three control modes. According to the stability criterion and to provide a sound dynamic performance, these compensated open-loop gains K should satisfy the following relationship:

$$K \leq \omega\xi \tag{21}$$

where ξ and ω are the damping ratio and hydraulic natural frequency, respectively. Therefore, there are

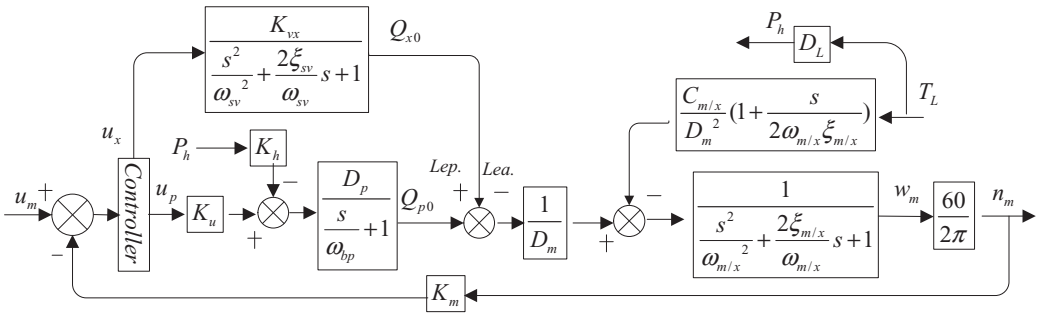

Figure 2. System block diagram in three control modes (subscript "*m/x*" represents "*m* or *x*", and "*x*" represents "*r*" and "*l*", respectively).

$K_1 \leq \omega_m \xi_m$, $K_2 \leq \omega_l \xi_l$ and $K_3 \leq \omega_r \xi_r$. The internal gains K_{mI}, K_{lI} and K_{rI} could be set using the aforementioned stability criterion.

The static closed-loop speed stiffness in the VSPC mode, LPVC mode and RPVC mode are, respectively, given by

$$\left|\frac{T_L}{n_m}\right|_m = \frac{K_1 {D_m}^2}{C_t} \tag{22}$$

$$\left|\frac{T_L}{n_m}\right|_l = \frac{K_2 {D_m}^2}{C_l} \tag{23}$$

$$\left|\frac{T_L}{n_m}\right|_r = \frac{K_3 {D_m}^2}{C_r} \tag{24}$$

4. Dynamic response analysis by simulation

4.1. Simulation model on AMESim

Figure 3 shows the simulation model used for the valve–pump parallel control in AMESim, which is a professional multidisciplinary simulation software routine, widely applied in hydraulics, automation and so on [22]. This software can help the researcher to rapidly establish hydraulic models to study dynamic performances by simulation. In general, to complete a simulation, four steps are required: sketch, choose submodels, set parameters and implement them.

The key components of AMESim are listed in Table 2. FP04 is used to set the characteristics of the hydraulic fluid, in which the effective bulk modulus is 1400 MPa. To simulate the total leakage from the pump and motor C_t, a fixed orifice is installed between two chambers of the hydraulic motor and is set to 1 L/(min MPa). The rated voltage of the inverter is set to 10 V corresponding to the maximum speed of the electric motor. The rated voltage of the PDV is set to 10 and −10 V corresponding to the maximum positive opening and negative opening, respectively. The initial voltage of the PDV is, respectively, set to 0 and −5 V (representing −50% pre-opening) when the system runs in the RPVC mode and LPVC mode. Many types of loads, such as sinusoidal load, ramp load, step load and square load, are applied to the system by setting different inputs to the PRV. A controller, which could switch between VSPC, LPVC and RPVC modes, is built.

Table 2. Parameters of key components.

Components	Specification
Electric motor	Power: 7.5 kW Rated speed: 3000 r/min
Inverter	Power: 11 kW with vector control Frequency range: 0.1–400 Hz
Pump	Displacement: 12 mL/r Speed range: 500–3000 r/min
Hydraulic motor and loading pump	Speed range: 0–90 r/min Displacement: 468 mL/r Rated pressure: 40 MPa
PDV	Rate flow: 9 L/min at 1.5 MPa Per-notch frequency: 60 Hz Damping ratio: 0.7
PRV	Pressure range: 0.7–31.5 MPa Rate flow: 200 L/min Inertia: 70 kg m^2

4.2. Dynamic response to control inputs

4.2.1. In open-loop control

Figure 4 shows that the parallel valve control has important effects on the total leakage coefficients and damping ratios. Figure 4(a) shows the control inputs of the inverter and PDV: at 0–5 s, the system is in the single pump control mode; from 5 to 15 s, the system is in the parallel valve control mode; after 15 s, all inputs remain constant. Figure 4(b) shows that, compared to the single pump control, the total leakage coefficients in parallel valve control become larger and vary with control inputs, because the total leakage coefficients in LPVC and RPVC, respectively, increase from C_t to $C_l = C_t + K_{cl}$, $C_r = C_t + K_{cr}$ due to the introduction of valve control. The total leakage from the pump and motor C_t values are small and constant, whereas the flow-pressure coefficients K_{cl} and K_{cr} are much greater and increase with valve inputs u_l and u_r according to $K_{cl} = \frac{C_{sv} u_l}{2\sqrt{P_h}}$, $K_{cr} = \frac{C_{sv} u_r}{2\sqrt{P_s - P_h}}$.

This change in the total leakage coefficients due to valve inputs will bring about positive and negative effects.

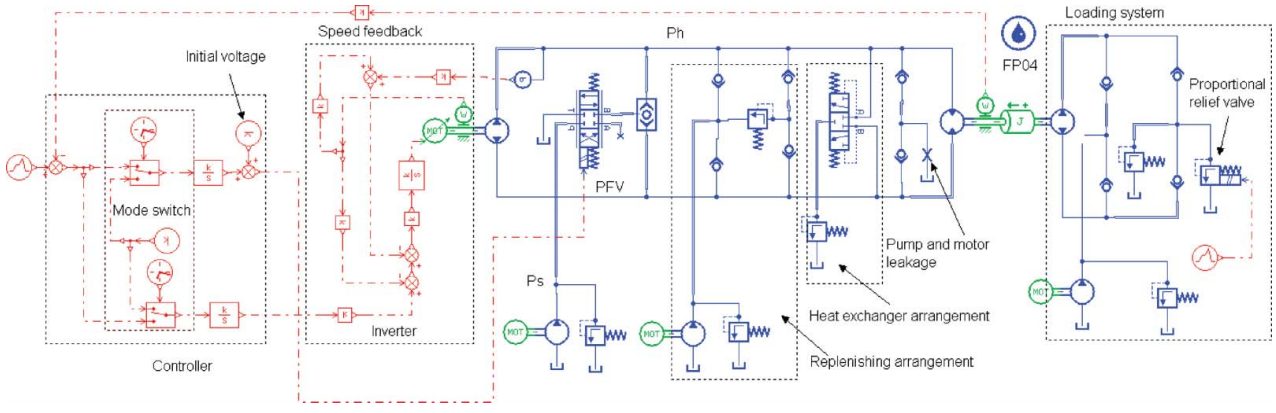

Figure 3. Simulation model on AMEsim.

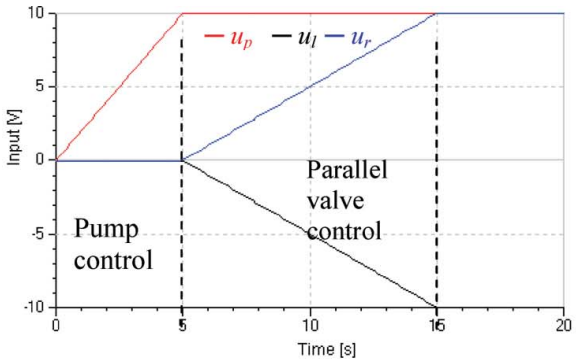

(a) Input signal of inverter and PDV

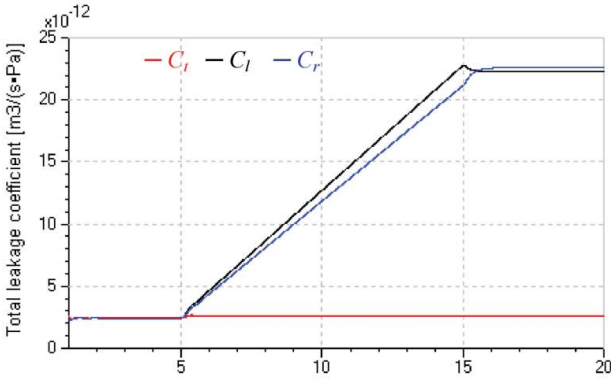

(b) Total leakage coefficients

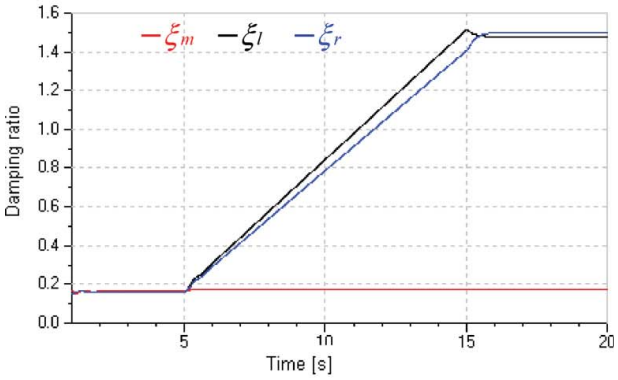

(c) Damping ratios

Figure 4. Influences of pump and valve inputs on total leakage coefficients and damping ratios (P_h = 10 MPa).

The positive effect consists in that damping ratios in parallel valve control become much greater than those in the single pump control, which could be proved by Figure 4(c). The change will benefit the dynamic response and system stability according to the system stability criterion: $K_2 \leq \omega_l \xi_l$, $K_3 \leq \omega_r \xi_r$.

The negative effect consists in that damping ratios vary widely with valve inputs and even can exceed 1 as shown in Figure 4(c). Furthermore, the system speed stiffness decreases and the hydraulic motor speeds are more susceptible to loads with the increase of valve input as shown in Figure 5. The decreasing speed stiffness and wide variation of damping ratios will cause more difficulties in control and prediction of the parallel control system.

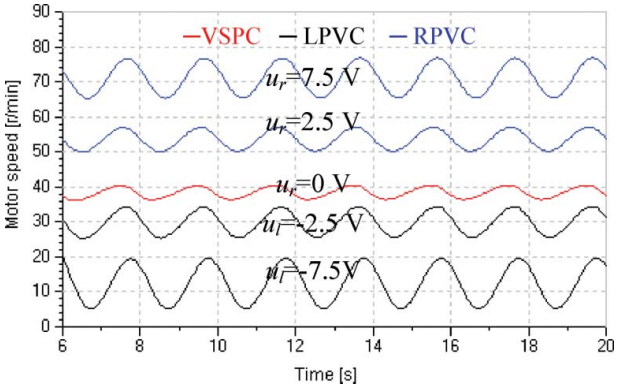

Figure 5. Influences of valve input on hydraulic motor speed (P_L = 5 + 3 sin0.5t MPa).

4.2.2. *In closed-loop control*

Figure 6 shows the step response of hydraulic motor speed under a constant load, and it is obvious that the parallel valve control systems respond faster than the pump controlled systems. There are two reasons: first, the three-servo system has the same natural frequency, i.e. $\omega_m = \omega_l = \omega_r$, as shown in Equations (11)–(13); second, referring to Equations (1) and (7), because $\omega_{sv} \gg \omega_{bp}$, the control valve responds much faster than the variable-speed pump (actually the inverter) and can control the flow more rapidly.

Figure 6 also shows that the response in the RPVC mode will be further improved by raising the supply pressure P_s. As known, the open-loop gain increase will accelerate the system response, and open-loop gains K_3 are proportional to flow gains K_{vr} according to Equation (20) and the flow gain of PDV in the replenishing status is given by $K_{vr} = C_{sv}\sqrt{P_s - P_h}$ in Equation(6), hence the raising P_s will increase K_{vr} and K_3 and then will accelerate the dynamic response.

4.3. *Dynamic response to load variation*

4.3.1. *In open-loop control*

Figure 7 shows influences of load variation on the total leakage coefficient when keeping the inputs of pump and valve constant (u_p = 6V, u_l = −4V, u_r = 4V).

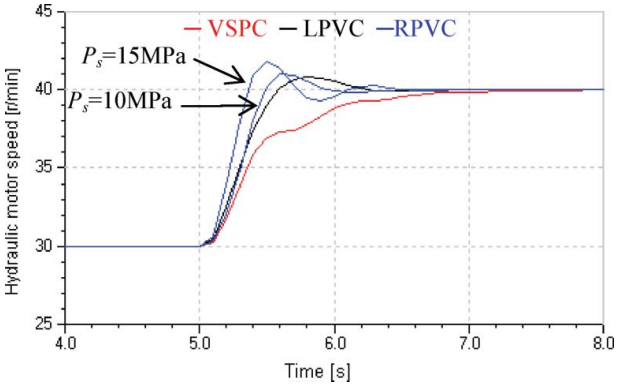

Figure 6. Step responses of hydraulic motor speed under a constant load.

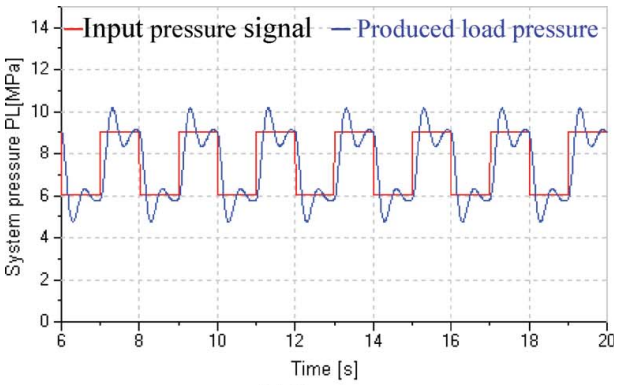

(a) Load pressure

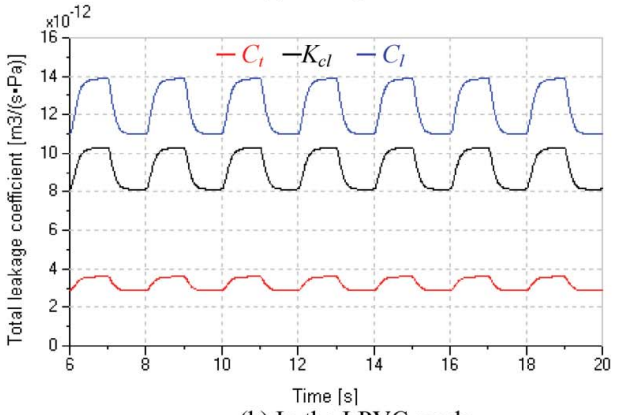

(b) In the LPVC mode

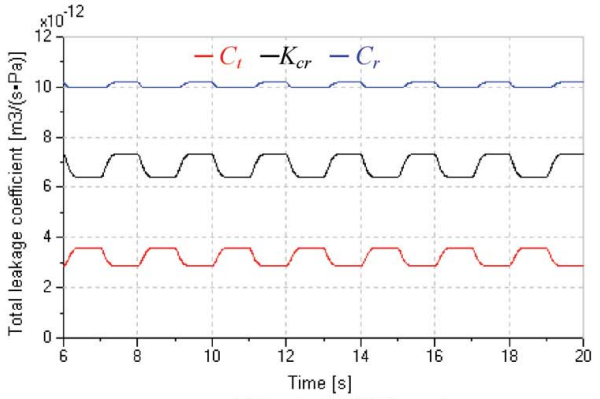

(c) In the RPVC mode

Figure 7. Total leakage coefficients under variable loads.

Figure 7(a) shows a square type of load pressure produced by a square-wave signal putting into a PRV. Comparing Figure 7(b,c), we can see that C_r is more constant with less variation than C_l, so the system under RPVC mode has more stable total leakage coefficients because K_{cr} and C_t have contrary tendencies to vary under RPVC mode, but K_{cl} and C_t have the same variation tendency in the LPVC mode. In addition, $C_l = C_t + K_{cl}$ and $C_r = C_t + K_{cr}$. We could find the answer from the expressions of C_t, K_{cl} and K_{cr}, i.e. $C_t = \frac{Q_{pm}}{2\sqrt{P_h}}$, $K_{cl} = \frac{C_{sv}u_l}{2\sqrt{P_h}}$, $K_{cr} = \frac{C_{sv}u_r}{2\sqrt{P_s - P_h}}$. In these expressions, both C_t and K_{cl} vary inversely with P_h, but K_{cr} is proportional to P_h.

The influences of total leakage coefficient variation due to load variation are as follows:

For the damping ratios, Figure 8(a) shows that damping ratios in the RPVC mode are smaller and

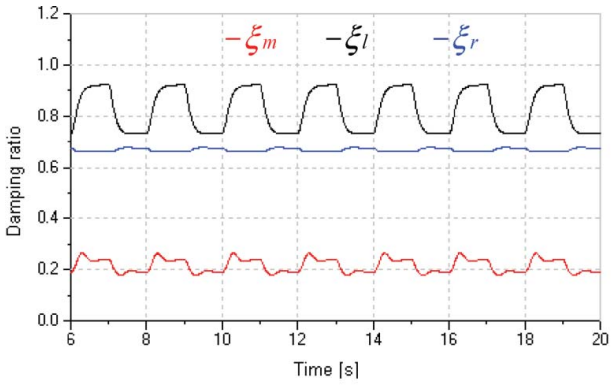

(a) Damping ratios

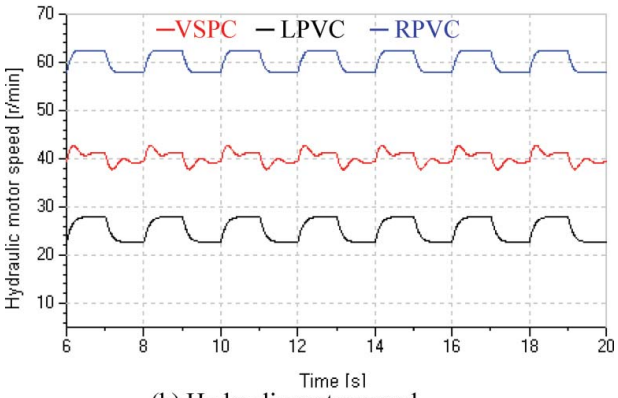

(b) Hydraulic motor speed

Figure 8. Damping ratios and hydraulic motor speed under variable loads.

more stable than that in the LPVC mode, which helps the system prediction and control.

For system speed stiffness, Figure 8(b) shows that the system in the RPVC mode has stronger speed stiffness and is less sensitive to load variation than that in the LPVC mode. In addition, as shown in Figure 9, speed stiffness in the RPVC mode could be further improved by raising the supply pressure P_s, that is because raising P_s will reduce K_{cr} and then C_r according to $K_{cr} = \frac{C_{sv}u_r}{2\sqrt{P_s - P_h}}$ and $C_r = C_t + K_{cr}$.

These trends seen in open-loop control remain available for a closed-loop control.

4.3.2. *In closed-loop control*

Step responses to step loads in a closed-loop control in three control modes are shown in Figure 10, which indicate the following dynamic properties:

(1) Speed stiffness in the parallel valve control is lower than that in the pump control because speed stiffness is inversely proportional to the total leakage coefficients according to Equations (22)–(24), and total leakage coefficients in parallel valve control are much larger than that in single pump control, i.e. $C_t < C_r$ and $C_t < C_l$ in Figure 10(b).

(2) System parameters in the RPVC mode are more stable than in the LPVC mode. Figure 10(b,c)

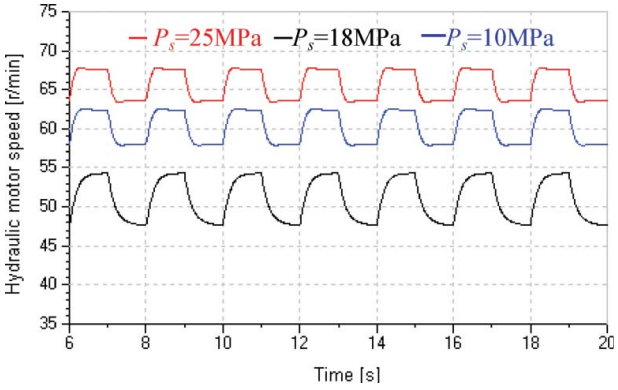

Figure 9. Hydraulic motor speed in RPVC under different P_s.

shows that total leakage coefficients and damping ratios in the LPVC mode vary widely, e.g. the damping ratio changes from 1.6 to 0.5, but those in the RPVC mode are more reasonable and constant, e.g. the damping ratio is about 0.5.

(3) Parallel valve control responds faster to load variation than pump control because of the rapid response of the PDV.

(4) The system in the RPVC mode is less susceptible to load variation compared with that in the LPVC mode. As shown in Figure 10(a), the system in LPVC responds quickly with only small-speed drops at a high pressure (e.g. at 10 s) and responds slowly with large-speed drops at a low pressure (e.g. at 6 s), even slower than that in pump control. The reason is as follows: according to $K_{cl} = \frac{C_{sv}u_l}{2\sqrt{P_h}}$, P_h is inversely proportional to K_{cl}, so a small P_h produces a large K_{cl}, C_l and ξ_l. In addition, ξ_l exceeds 1 at 6 s in Figure 10(c), which decelerates the response and increases the settling time. However, the system in the RPVC mode has small and constant total leakage coefficients and damping ratios.

Figure 11 shows that the system in the RPVC yielded two benefits by increasing the supply pressure P_s:

(1) Accelerating dynamic response. According to the valve flow gain $K_{vr} = C_{sv}\sqrt{P_s - P_h}$ and Equation (20), increasing P_s will increase K_{vr} and open-loop gain K_3 and increasing K_3 will contribute to the system-response improvement.

(2) Improvement of closed speed stiffness. Referring to flow-pressure coefficient $K_{cr} = \frac{C_{sv}u_r}{2\sqrt{P_s - P_h}}$, increasing P_s will reduce K_{cr} and C_r, and increasing K_3 and reducing C_r will enhance the closed-loop stiffness according to Equation (24).

Furthermore, for the same valve opening, $K_{vr} > K_{vl}$ and $K_3 > K_2$ when $P_s > 2P_L$, so the system in RPVC mode will respond faster with a higher closed stiffness than that in LPVC mode; however, the system in the

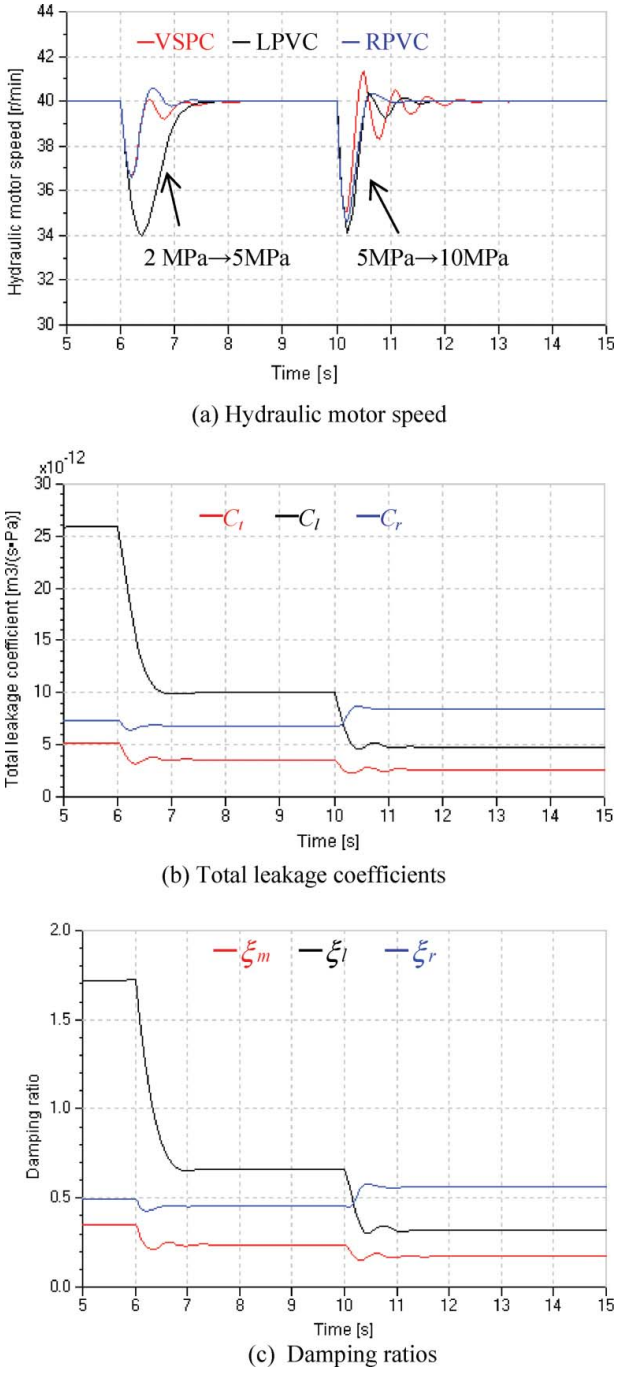

Figure 10. Responses for step loads.

LPVC mode does not have such an advantage, because when the PDV works in the leaking status, both its flow gain $K_{vl} = C_{sv}\sqrt{P_h}$ and flow-pressure coefficient $K_{cl} = \frac{C_{sv}u_l}{2\sqrt{P_h}}$ just relate to P_h not P_s, and P_h only depends on load and could not be manually adjusted.

5. Experimental verification

5.1. Experimental system

To verify the availability of RPVC and LPVC, a parallel valve control experimental system as shown in Figure 12 is established based on the principle in Figure 1, control model in Figure 2 and parameters in Tables 1 and 2. Main system parameters are as

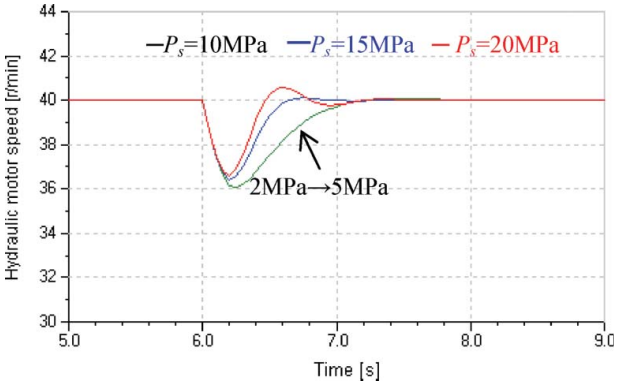

Figure 11. Hydraulic motor speed response for step loads in the different P_s.

follows: the rated system pressure is 20 MPa, the rated flow is 50 L/min (the rated flows of the pump and valve are 40 and 10 L/min, respectively), the maximum motor speed of is 90 rpm, the oil replenishing pressure is 0.8 MPa, the flushing overflow pressure is 0.5 MPa and the tank volume is 800 L (air-cooled). Figure 13 shows the loading system, the left hydraulic motor drives the rotary inertia and the right hydraulic motor is used to load under regulation of its outlet pressure by a proportional pressure relief valve. The total weight of the rotary inertia is 900 kg, the rotating diameter is 750 mm and the total inertia is 72 kg m^2. The inertia block by modular design includes five small blocks: the basic one is 24 kg m^2 and the other four ones have 12 kg m^2. The measurement and control system is developed based on the Labview platform in Figure 14. System pressures, flow rates and rotary speeds are measured by various types of sensors logged on to an industrial computer via the data acquisition card. After data processing, the acquisition card outputs control signals to the inverter, PDV and PRV to achieve the pump–valve parallel control. The system has the functions of data acquisition, data processing, control, display and storage, and could be used to conduct various experiments in different modes such as VSPC, RPVC and LPVC.

To verify the validity of parallel valve control in improving the response of VSPC systems, step-

Figure 12. Experimental system.

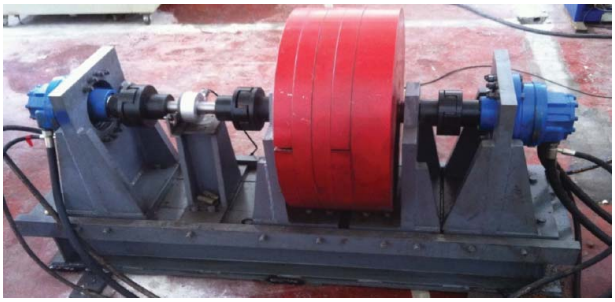

Figure 13. Loading system.

response experiments are carried out in the VSPC, LPVC and RPVC modes, respectively. All experiments are carried out in closed-loop control, and every experiment is repeated two or three times. From Section 4, the system in the three control modes is a Type 0 system and unstable before compensation. PI compensation is applied to the control system, and its transfer function is

$$G_c(s) = K_p\left(1 + \frac{1}{T_i s}\right) = K_p + \frac{K_I}{s} \tag{25}$$

where K_p is the proportional gain, T_i is the internal time, K_I is the internal gain and $K_I = K_p/T_i$. So K_I is defined by K_p and T_i. Optimal PI parameters through many experiments are obtained (shown in Table 3), and there is always a relationship, $K_I \gg K_p$ in three control modes, so the PI compensation can be considered as an internal compensation mechanism, as discussed in Section 4. The following experiment results indicate that these PI configurations in different control modes are reasonable.

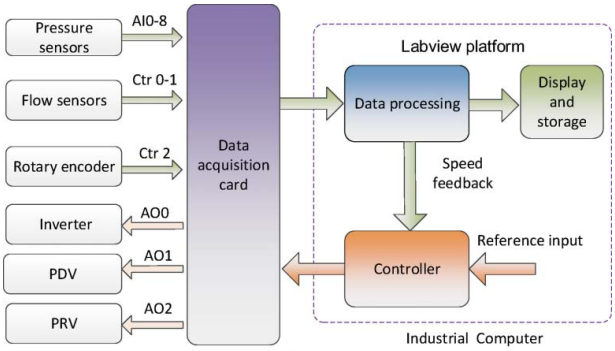

(a) Principle

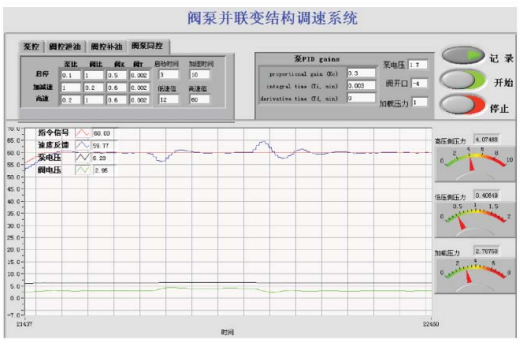

(b) Interface

Figure 14. Measurement and control system.

Table 3. Coefficients of PI in the different modes.

Control mode	K_p	T_i	K_I
VSPC	0.3	0.18	1.67
LPVC	0.6	0.12	5
RPVC	0.7	0.12	5.8

5.2. In the LPVC mode

For the step-response experiments in the LPVC mode, we make the following sets: $u_p = 7.2$ V, and then the variable-speed pump becomes a fixed-speed pump and supplies a basic flow for the control system and the control valve works in the leaking status with an initial opening corresponding to $u_{l0} = -6$ V. Figure 15 shows the step response to control inputs in the LPVC and VSPC modes, and it is clear that it responds in the LPVC mode faster than in the VSPC mode because the control valve responds much faster than the variable-speed pump.

5.3. In the RPVC mode

For the step-response experiments in the RPVC mode, the following configurations are used: $u_{p0} = 5.1$ V, and then the variable-speed pump becomes a fixed-speed pump and supplies a basic flow for the control system, and the control valve works in the replenishing status with an initial opening corresponding to $u_{r0} = 1$ V. Figure 16 shows the step response to control inputs in the RPVC and VSPC modes, and we can obtain the following characteristics of the RPVC system from the figure.

(1) Compared to the system in the VSPC mode, the one in the RPVC mode responds much faster and with a shorter adjusting time. This can be verified by the hydraulic motor speed step response at speeds of 55 and 65 rpm.

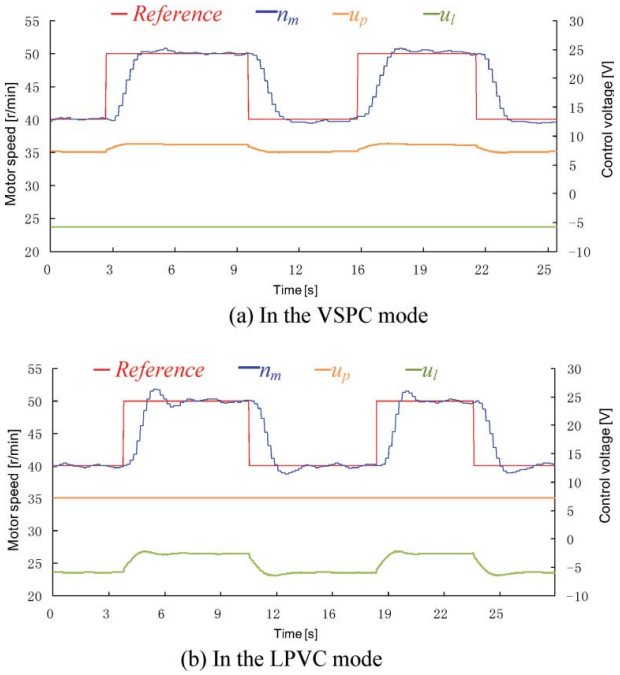

(a) In the VSPC mode

(b) In the LPVC mode

Figure 15. Step response for reference in the VSPC and LPVC modes.

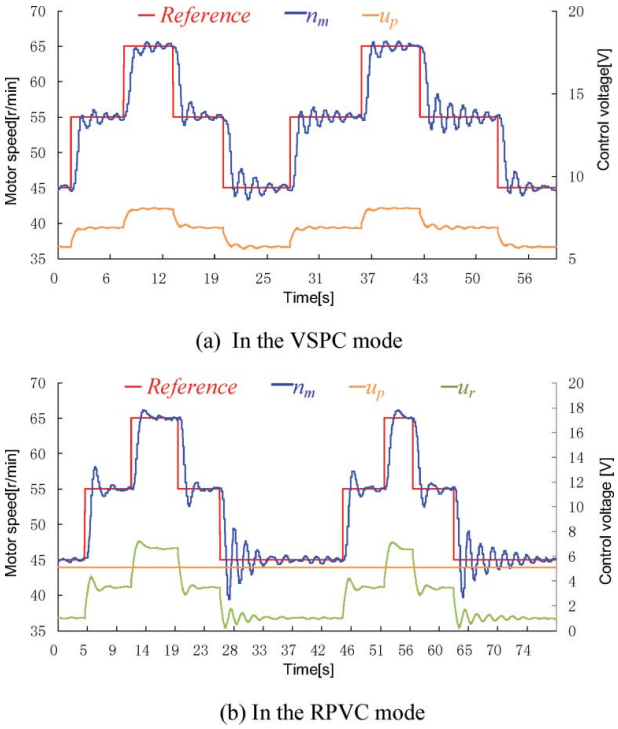

(a) In the VSPC mode

(b) In the RPVC mode

Figure 16. Step response for reference in the RPVC and VSPC modes.

(2) Compared to the system in the VSPC mode, the one in the RPVC mode has greater damping ratios which vary widely with a valve control voltage. This can be validated from two speed step responses from 45 to 55 rpm and from 55 to 65 rpm. It is obvious that the overshoot at 65 rpm is much smaller than that at 55 rpm. This is because the overshoot decreases with the increasing damping ratios which increase with valve voltage and the valve voltage at 65 rpm is greater than that at 55 rpm.

Figure 17 shows the influence of variation of PI parameters in the RPVC and VSPC modes. It is obvious that compared with the VSPC system, the one in the RPVC mode has a large control margin and is only slightly susceptible to variations in the PI parameters. This is because the damping ratios in the RPVC mode become large, which makes the right-hand side of (21) to increase, and becomes more easily satisfied, even if the proportional gain K_p varies widely.

Figure 18 shows the influence of different P_s and PI parameters to system response in the RPVC mode, which also indicates two characteristics of RPVC:

(1) Greater P_s contributes to a faster response in the same PI parameters, but too great a P_s may cause too large an overshoot and even may lead to the system instability.

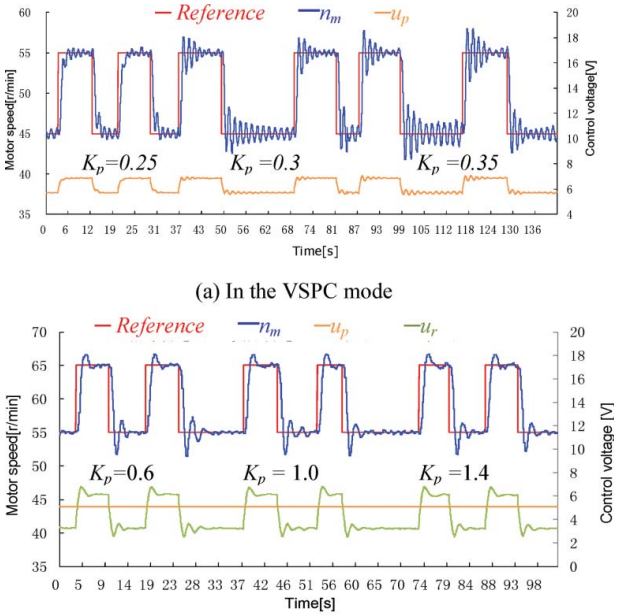

(a) In the VSPC mode

(b) In the RPVC mode

Figure 17. Influence of variation of PI parameters in the VSPC and RPVC modes.

(2) To obtain a good response, P_s should match the PI parameters, for example, large P_s corresponding to small K_p.

The specific reasons are as follows: according to valve flow gain $K_{qr} = C_{sv}\sqrt{P_s - P_h}$ and system open-loop gain $K = 60K_IK_mK_{qr}/(2\pi D_m)$, increasing P_s will increase K_{qr} and K, which helps to improve the system response. However, too large P_s leads to too large K and will cause (21) to be difficult to be satisfied, thus degrading the system stability.

Results of experiments and simulation prove that the LPVC and RPVC indeed help to improve the system response.

6. System efficiency analysis

In the previous sections, the system dynamic response in three control modes is considered, and the system efficiency will be analyzed in this section. The power of hydraulic systems is the product of the pressure and flow, and pressure varies with loads; so the system energy is essentially controlled by flow rates. In the valve–pump parallel control system, the system flow (ignoring system leakages) is given by

$$Q_s = Q_p \pm Q_v \tag{26}$$

where Q_s is the system flow and is also the input flow of hydraulic motor; there is $Q_s = Q_p + Q_v$ in the RPVC mode and $Q_s = Q_p - Q_v$ in the LPVC mode.

There are two basic control modes in this parallel control system, i.e. pump control and valve control. Pump control is more efficient since both flow and

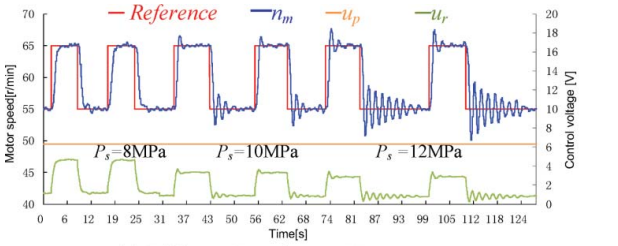

(a) Different P_s and same PI parameters

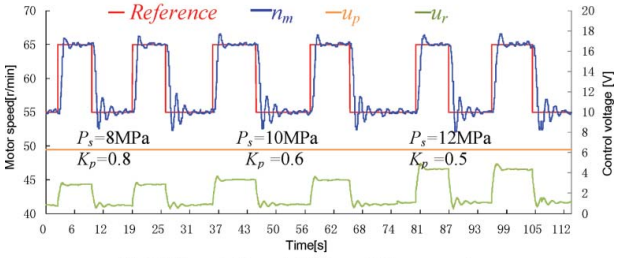

(b) Different P_s and different PI parameters

Figure 18. Influence of different P_s and PI parameters to system response in the RPVC mode.

pressure are closely matched with the load demand without any throttling loss, but the valve control is less efficient because of the unavoidable throttling loss. Therefore, the system energy loss is mainly the throttling loss resulting from valve control, and the system efficiency is

$$\begin{cases} \eta = \dfrac{N_m}{N_v + N_m} \\ N_v = \Delta p \times Q_v \\ N_m = Q_s \times P_L \\ K_{pv} = Q_p/Q_v \end{cases} \tag{27}$$

where N_m is the output power of the hydraulic motor, P_L is the load pressure, N_v is the throttling loss due to the valve control, which increases with the valve control flow, Δp is the drop in pressure at the valve orifice and K_{pv} is the flow ratio of pump to valve flow rate. Combining Equations (26) and (27), the expression for system efficiency is obtained by

$$\eta = \frac{(K_{pv} \pm 1)P_L}{\Delta P + (K_{pv} \pm 1)P_L} \tag{28}$$

From Equation (28), we concluded that the ratio K_{pv} could be used to describe the system efficiency, and the greater K_{pv} is, the greater pump control flow is, and the lower the valve control flow is, the higher the system efficiency is.

Figure 19 shows the flow assignment to the pump and valve in closed-loop control under sinusoidal loads. Figure 19(a) shows that the variable-speed pump provides all flows and the valve only leaks a little in the LPVC mode, so $K_{pv} \approx 12$. Figure 19(b) shows that the variable-speed pump supplies the majority of the flow and the valve only supplies a little of the flow

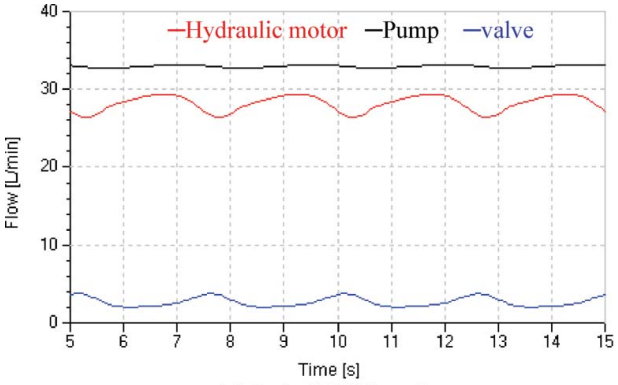

(a) In the LPVC mode

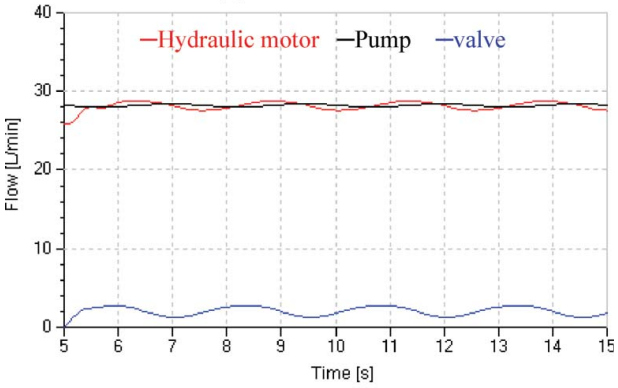

(b) In the RPVC mode

Figure 19. Flow assignment of pump and valve in closed-loop control under sinusoidal loads.

in the RPVC mode, hence $K_{pv} \approx 10$. So, two parallel control systems are characterized by a high-efficiency and rapid response. Moreover, K_{pv} will be higher, and the parallel control systems will be more efficient if the required maximum speed of the hydraulic motor increases because the corresponding flow is supplied by the pump, but not by the valve.

7. Conclusions

(1) After adding the valve control to pump control systems, the total leakage coefficients increase significantly and vary widely, which will increase damping ratios and reduce oscillations, as well as reduce velocity stiffness and make the system vulnerable to load disturbance.
(2) Both the LPVC and RPVC could contribute to the dynamic response improvement, but the system in RPVC has a more stable damping ratio which is conducive to system prediction and control. Moreover, these advantages could be further improved by increasing the supply pressure of the control valve. LPVC also has the advantage of low cost due to no need of the oil supply for the control valve.
(3) In the parallel valve control mode, the pump provides all (or the majority) of the system flow, and the valve only handles low flow rate; so parallel control systems still have relatively high-energy efficiency as pump control systems.

Disclosure statement

No potential conflict of interest was reported by the authors.

Funding

This work is supported by a project funded by the Priority Academic Program Development of the Jiangsu Higher Education Institutions and the Fundamental Research Funds for the Central Universities [grant number 2015QNA33].

References

[1] Merritt HE. Hydraulic control systems. New York (NY): Wiley; 1967.
[2] Manring ND. Hydraulic control systems. New York (NY): Wiley; 2005.
[3] Karunanidhi S, Singaperumal M. Mathematical modelling and experimental characterization of a high dynamic servo valve integrated with piezoelectric actuator. Proc IMechE, Part I: J Syst Control Eng. 2010;224 (4):419–435.
[4] Yutaka T, Tetsuji M, Kazuo N. Speed and displacement control of pump system for energy saving. In: Chen Zhaoneng, editor. Proceeding of 2nd International Symposium on Fluid Power Transmission and Control; Oct 5–7; Shanghai, China. Shanghai: Shanghai Scientific and Technological Literature Publishing House; 1995. p.12–16.
[5] Kazuo N, Yutaka T. Energy saving type electrohydraulic servo system. J Fluid Control. 1988;18(3):35–51.
[6] Yang HY, Yang J, Xu B. Computational simulation and experimental research on speed control of VVVF hydraulic elevator. Control Eng Pract. 2004;12(5):563–568.
[7] Wang YQ, Zhang W. The presence and development of fluid power transmission and control. Chin J Mech Eng. 2003;39(10):95–99.
[8] Naseradinmousavi P. A novel nonlinear modeling and dynamic analysis of solenoid actuated butterfly valves coupled in series. ASME J Dyn Syst Meas Control. 2015;137(1):14505-1–14505-5.
[9] Naseradinmousavi P, Machiani SG, Ayoubi MA, et al. Coupled operational optimization of smart valve system subject to different approach angles of a pipe contraction. Struct Multidisc Optim. 2017;55(3):1001–1015.
[10] Naseradinmousavi P, Segala DB, Nataraj C. Chaotic and hyperchaotic dynamics of smart valves system subject to a sudden contraction. ASME J Comput Nonlinear Dyn. 2016;11(5):51025-1–51025-9.
[11] Manasek R. Simulation of an electro-hydraulic load-sensing system with AC motor and frequency changer. In: Scheidl R, Sobczyk A, editors. Proceeding of 1st FPNI-PhD Symposium; Sep 20–22; Hamburg, Germany. Hamburg: Technical University of Hamburg; 2000. p. 314–324.
[12] Shen HK, Jin B, Chen Y. Research on variable speed electro-hydraulic control system based on energy regulating strategy. In: Proceeding of ASME International Mechanical Engineering Congress and Exposition; Nov 5–10; Chicago, IL. New York: ASME; 2006. p. 230–236.

[13] Shen HK, Jin B, Chen Y. Variable speed hydraulic control system based on energy regulation strategy. J Mech Eng. 2009;45(5):210–213.
[14] Jin B, Shen HK, Chen Y. Energy-regulation based variable speed hydraulic cylinder position control system. J Mech Eng. 2008;44(1):25–30.
[15] QI XY, Fu YL, Wang ZL. Scheme analysis of power-by-wire airborne actuation system. J Beijing Univ Aeronaut Astronautics. 1999;25(4):426–430.
[16] Cochoy O, Hanke S, Carl UB. Concepts for position and load control for hybrid actuation in primary flight controls. Aerosp Sci Technol. 2007;11(3):194–201.
[17] Kang RJ, Jiao ZX, Wang SP. Design and simulation of electro-hydrostatic actuator with a built-in power regulator. Chin J Aeronaut. 2009;22(6):700–706.
[18] Ding HG, Zhao JY. Performance analysis of variable speed hydraulic systems with large power in valve-pump parallel variable structure control. J Vibroeng. 2014;16(2):1065–1085.
[19] Ding HG, Zhao JY, Li GZ. Analysis of valve-pump combined high power hydraulic speed regulation schemes. J China Coal Soc. 2013;38(9):1703–1709.
[20] Ding HG, Zhao JY. A new method of improving low-speed performance of variable speed hydraulic systems: by leaking parallel valve control. Adv Mech Eng. 2014;10.
[21] Ding HG, Zhao JY, Zhao L. Analysis on electrohydraulic speed servo control schemes for anti-explosion hydraulic hoisters. J China Coal Soc. 2011;36(8):1407–1411.
[22] Alessandro R, Salvatore M, Nicola N. Modelling of variable displacement axial piston pump in a multi-body simulation environment. ASME J Dyn Syst Meas Control. 2007;129(4):456–468.